Geosciences **2013**, *3*, 502-527; doi:10.3390/geosciences3030502

OPEN ACCESS

geosciences

ISSN 2076-3263

www.mdpi.com/journal/geosciences

Article

Provenance of Late Paleozoic-Mesozoic Sandstones, Taimyr Peninsula, the Arctic

Xiaojing Zhang [1,*], Jenny Omma [2,†], Victoria Pease [1] and Robert Scott [2,‡]

[1] Department of Geological Sciences, Stockholm University, Stockholm 106 91, Sweden; E-Mail: vicky.pease@geo.su.se

[2] CASP, Department of Earth Sciences, University of Cambridge, Cambridge CB3 0DH, UK; E-Mail: jenny.omma@gmail.com (J.O.); robert.scott@casp.cam.ac.uk (R.S.)

† Current address: BP Exploration Operating Co. Ltd., Chertsey Road, Middlesex TW16 7LN, UK.

‡ Deceased on 26 September 2012.

* Author to whom correspondence should be addressed; E-Mail: xiaojing.zhang@geo.su.se; Tel.: +46-8-674-7824; Fax: +46-8-674-7897.

Received: 4 May 2013; in revised form: 11 July 2013 / Accepted: 15 July 2013 / Published: 29 July 2013

Abstract: The sedimentary and provenance characteristics of seven Permo-Carboniferous and two early Cretaceous samples from the Taimyr Peninsula provide information about the latest evolution of Uralian orogeny and the opening of the Amerasian Basin. The Permo-Carboniferous samples have a mixed provenance of recycled and first cycle sediment, sourced from metamorphic and igneous terranes. U-Pb detrital zircon ages represent a mixture of Precambrian-Paleozoic grains with euhedral, penecontemporaneous late Carboniferous and Permian grains consistent with derivation from the Uralian Orogen, plus additional Timanian and Caledonian material presumably derived from Baltica. Differences between the late Permian sample and the other Carboniferous and early Permian samples are interpreted to reflect the final collisional stage of Uralian orogeny. Early Cretaceous sediments deposited at the time of the Amerasian Basin opening preserve a mixed provenance of mainly first cycle metamorphic and igneous source material, as well as an unstable heavy mineral assemblage dominated by staurolite, suggesting local derivation. Detrital zircon ages fall almost exclusively into one late Permian-early Triassic cluster, indicating a Siberia Trap-related magmatic source. The detrital zircon age spectra support a passive margin setting for Taimyr during the opening of the Amerasian Basin in the early Cretaceous.

Keywords: provenance; heavy minerals; detrital zircons; Uralian Orogen; Amerasian Basin

1. Introduction

Several orogens, including the Uralian Orogen, extend into the Arctic, but are lost beneath its seas. The Ural Mountains represent the late Paleozoic collision between Baltica, Kazakhstan and Siberia [1–3] as the final stage of the assembly of Pangaea [4–7] and is believed to have played an important role in the tectonic evolution of the Eurasian Arctic continental margin [8]. The Urals can be traced over 2000 km, from the Aral Sea in the south to the Arctic. However, the Arctic continuation of the Uralian Orogen beyond the Polar Urals is highly debated (e.g., [9–12]). Some authors argue that the orogen terminates at the Polar Urals [13,14], while others have suggested it continues northward to the Taimyr Peninsula [15,16] or bends along Pay Khoi to Novaya Zemlya, then to Taimyr, Severnaya Zemlya and, at last, back into the Asian mainland [17] (Figure 1a).

Figure 1. (**a**) Regional setting of the Taimyr Peninsula. Bathymetry is from the International Bathymetric Chart of the Arctic Ocean (IBCAO) database [18]. Note the possible scenarios for the northward continuation of the Urals; (**b**) simplified geological map of the Taimyr Peninsula (after Bezzubtsev *et al.* [19]; Inger *et al.* [20]). Circles indicate sample localities. Question marks indicate different opinions for the possible continuation of the Arctic Uralides (refer to text for details).

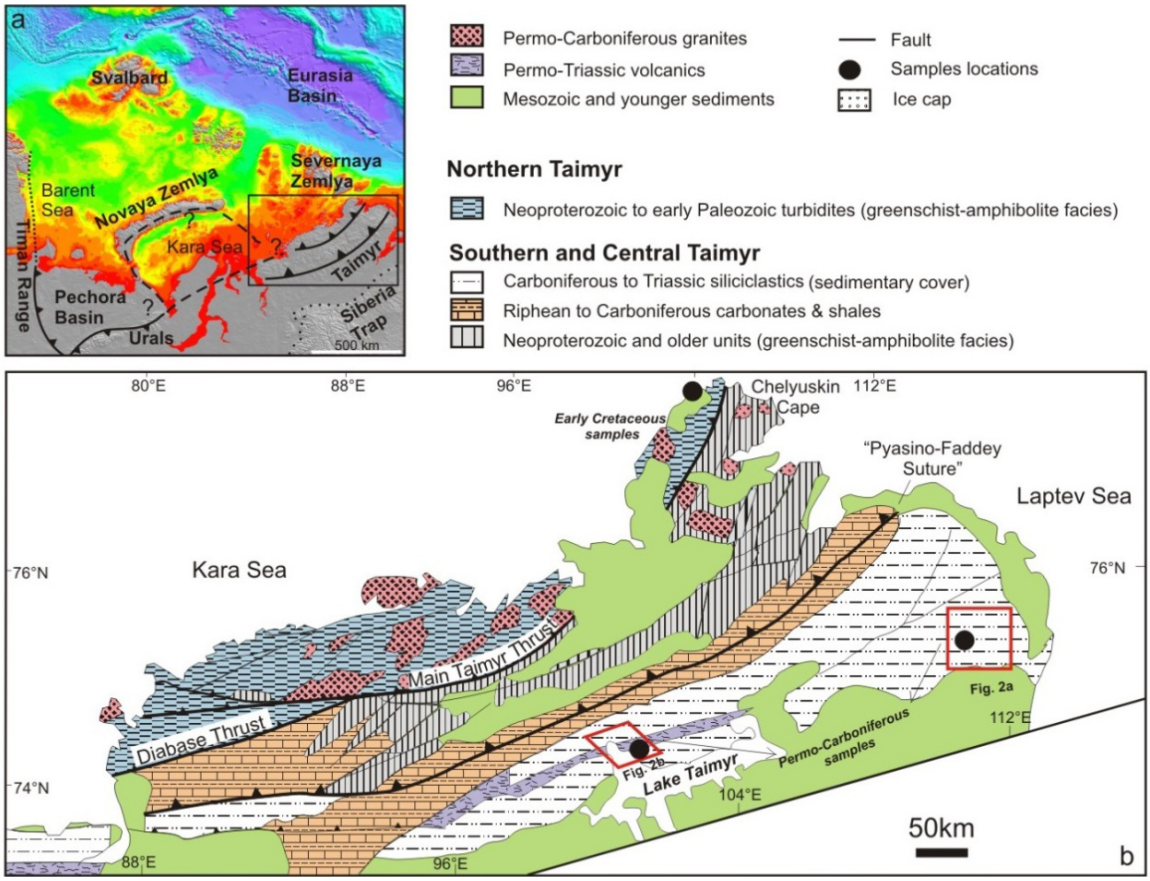

The Taimyr Peninsula is a key element in testing different hypotheses regarding the northward continuation of the Uralian Orogen. Southern Taimyr represents the passive margin of Siberia and is dominated by a Paleozoic to early Mesozoic succession [20,21]. This siliciclastic package records the influx of detritus generated by a late Paleozoic event, which may be linked to the latest stage of Uralian Orogenesis when the so-called Kara Block collided with Siberia. The Kara Block comprises Northern Taimyr and Severnaya Zemlya (Figure 1a), and a growing body of evidence suggests that the Kara Block was a part of Baltica since the late Neoproterozoic [22–26]. Provenance investigations of Permo-Carboniferous sediment in Taimyr can determine the geologic affinities of these successions and provide information about the northern extent of contemporaneous Uralian orogenesis.

Permian/Triassic plume-related (Siberian trap) magmatism [27] represents the onset of crustal extension and associated rifting, followed by Mesozoic and Cenozoic sedimentation [28–30]. The Taimyr Peninsula underwent dextral transpression associated with uplift and erosion between Triassic rifting and thermal subsidence in Jurassic and Cretaceous times [20,21,31]. Early Cretaceous sedimentation is coeval with the opening of the Amerasian Basin [7,32], and thus, provenance studies of early Cretaceous samples may provide information about the geological setting of Taimyr during the development of the Amerasian Basin. We present detrital zircon U-Pb ages combined with petrography and heavy mineral data to determine the provenance of the late Paleozoic and early Cretaceous strata of Taimyr in order to address these questions.

2. Geological Setting

The Taimyr Peninsula lies north of the Siberian craton and is bounded by the Laptev Sea to the east and the Kara Sea to the north and west (Figure 1a). It is generally divided into three NE–SW trending domains (Figure 1b) [33]. Southern Taimyr contains a weakly to unmetamorphosed Ordovician to mid-Carboniferous carbonate-dominated passive margin shelf succession of the Siberia Craton [20,31,34]. The passive margin succession is overlain by late Carboniferous to early Triassic shallow-marine and continental siliciclastic rocks interlayered with Permian–Triassic extrusive and intrusive rocks of the Taimyr igneous suite [20,21]. This siliciclastic package records an influx of continental detritus, possibly caused by erosion of the developing late Paleozoic collision between Baltica and Siberia to the west and north. Rare thrust faults observed within the Paleozoic carbonate succession are considered to be late Paleozoic structures possibly related to late Paleozoic orogenesis [20]. During late Triassic to earliest Jurassic time, all of the Triassic and older rocks in southern Taimyr were folded and faulted during dextral transpression [20,21,31].

Central Taimyr is structurally and lithologically complex. It contains a varied assemblage of Precambrian basement. Greenschist facies Neoproterozoic crust predominates, including continental terranes and volcano-sedimentary successions, as well as fragmented ophiolites and island-arc volcanic rocks [35–37]. These Neoproterozoic units occur with Mesoproterozoic to early Neoproterozoic amphibolite-facies metasedimentary units, which were intruded by *ca.* 900 Ma granites [38]. Unconformably overlying the metamorphosed units is a weakly to unmetamorphosed latest Neoproterozoic (Vendian) to early Paleozoic continental margin succession, which is interpreted to be deposited on the continental slope of Siberia [20] and indicates that central-southern Taimyr has been a coherent part of

Siberia since at least the latest Neoproterozoic time. The Pyasino-Faddey Suture represents the contact between southern Taimyr and central Taimyr.

Northern Taimyr is dominated by interbedded Neoproterozoic and early Paleozoic sandstones, siltstones and mudstones, interpreted as continental slope turbidites [34]. These sediments were metamorphosed under regional greenschist to amphibolite facies conditions in the late Paleozoic. They were extensively intruded by Carboniferous to Permian age (300–265 Ma) syenites thought to represent syn- to post-tectonic magmatism [39–41]. The late Paleozoic suture lies along the SE-verging thrust contact (Main Taimyr Thrust) separating northern and central Taimyr. In the NE, undeformed late Jurassic and early Cretaceous coal measures overlie unconformably deformed Neoproterozoic to Paleozoic strata [19,34,36].

3. Samples and Methods

Permo-Carboniferous sandstone samples were collected from southern Taimyr near the eastern coast (VP10-12, VP10-14 and VP10-25) and in the vicinity of Lake Taimyr (RAS98-8, RAS98-9, RAS98-23 and RAS98-32). Cretaceous samples (RAS99-26, RAS99-32) were collected from northern Taimyr, at the coast of Chelyuskin Cape. Their geological and stratigraphic setting is shown in Figures 2 and 3 and Table 1. Samples VP10-25 and RAS98-23, were collected from the late Carboniferous to the early Permian Turozovskya Formation (C_3-P_1tr); samples RAS98-8, RAS98-9 and RAS98-32 were collected from the early Permian Byrrangskaya Formation (P_1br); sample VP10-14 was collected from the early Permian Sokolinskaya Formation (P_1sk); sample VP10-12 was collected from the late Permian Baykurskaya Formation (P_2bk). This Permo-Carboniferous sedimentary succession is composed of siltstones, sandstones, mudstones and conglomerates with layers of coal. Samples RAS99-26 and RAS99-32 were collected from an unnamed Cretaceous formation. The Jurassic-Cretaceous marginal marine strata are unconsolidated and flat-flying, unconformably overlying deformed Paleozoic and early Triassic units. The samples were petrographically evaluated and analyzed for heavy mineral composition and U-Pb ages of detrital zircon.

Table 1. Locations and stratigraphy of samples and methods used in this study.

Sample No.	Location	Formation	Petrography	Heavy mineral analysis	Detrital zircon geochronology
VP10-12	Southeastern Taimyr	Late Permian Baykurskaya	X	X	X
VP10-14	Southeastern Taimyr	Early Permian Sokolinskaya	X	X	X
VP10-25	Southeastern Taimyr	Late Carb to Early Permian Turozovskya	X	X	X
RAS98-8	Near Taimyr Lake	Early Permian Byrrangskaya	X	X	X
RAS98-9	Near Taimyr Lake	Early Permian Byrrangskaya	X	X	–
RAS98-32	Near Taimyr Lake	Early Permian Byrrangskaya	X	X	–
RAS98-23	Near Taimyr Lake	Late Carb to Early Permian Turozovskya	X	X	–
T99-26	Northern Taimyr	Early Cretaceous Unnamed	X	X	X
T99-32	Northern Taimyr	Early Cretaceous Unnamed	X	X	–

Figure 2. Geological map showing Paleozoic sample locations. (**a**) The eastern coast of southern Taimyr (after Bezzubtsev *et al.* [34]); (**b**) the vicinity of Taimyr Lake (after Bezzubtsev *et al.* [19]; Inger *et al.* [20]).

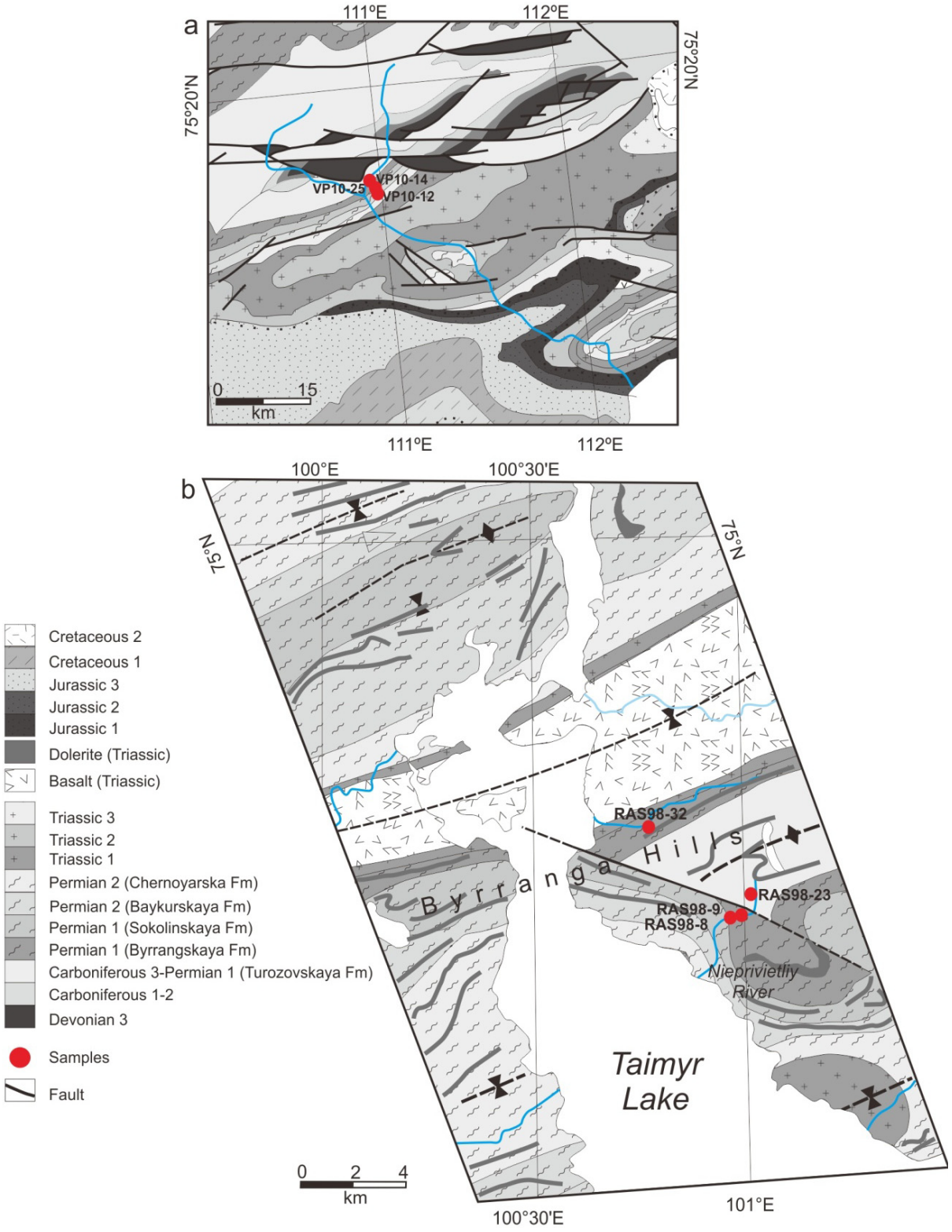

Figure 3. Partial stratigraphic column for Taimyr. Late Paleozoic stratigraphy of southern Taimyr is modified after Bezzubtsev *et al.* [19] and Inger *et al.* [20]. Mesozoic stratigraphy of northern Taimyr is modified after Natapov *et al.* [42]. The stratigraphic positions of the samples discussed in the text are shown.

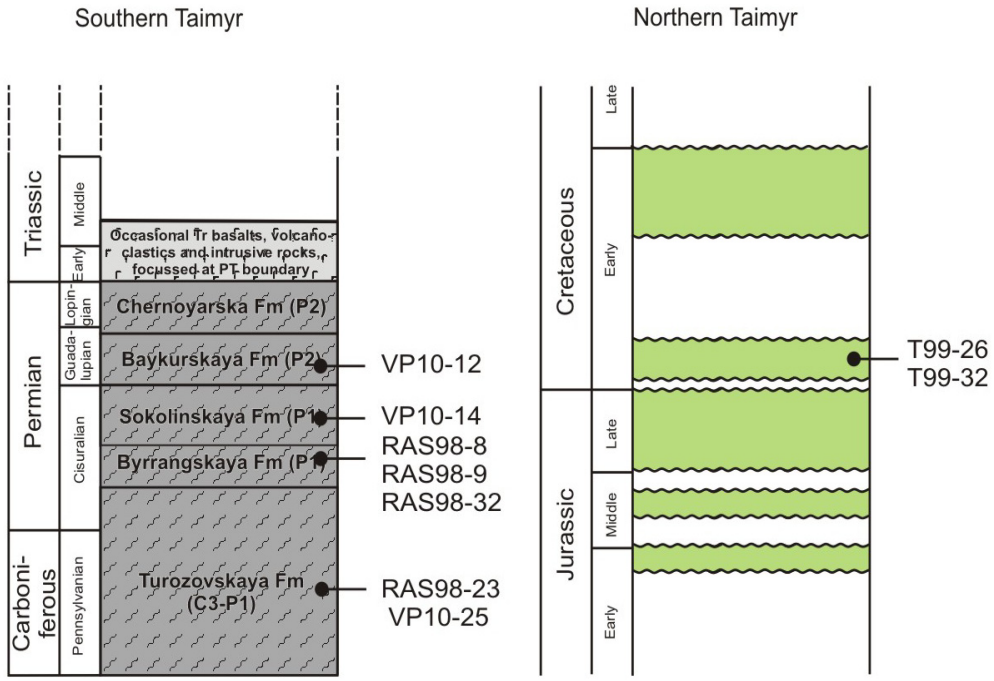

3.1. Petrography

Sandstone composition and maturity was assessed via point counting of thin sections to provide provenance information. 200–500 points were counted on each thin-section using the method proposed by Dickinson [43], with quartz, feldspar and lithic fragments as the main framework grains. The parameters and the results are listed in Table 2.

3.2. Heavy Mineral Analysis

Heavy mineral samples were prepared following the method of Mange *et al.* [44] and Morton *et al.* [45]. Samples were gently disaggregated using a pestle and mortar, avoiding grinding action. Chemical pre-treatment was avoided to prevent the possibility of modifying assemblages in the laboratory. Following disaggregation, the samples were immersed in water and cleaned by an ultrasonic probe to remove and disperse any clay that might have adhered to grain surfaces. The samples were washed through a 63 μm sieve and re-subjected to ultrasonic treatment until no more clay passed into suspension. At this stage, the samples were wet sieved through the 125 and 63 μm sieves, and the resulting >125 μm and 63–125 μm fractions were dried in an oven at 80 °C. The 63–125 μm fractions placed in Lithium heteropolytungstate (LST) with a measured specific gravity of 2.8 were put in a centrifuge at 3000 rpm for 15 min to separate heavy minerals. The heavy mineral residues were mounted under Canada balsam for optical study using a polarizing microscope. About 200 non-opaque detrital heavy mineral grains were counted in each sample to estimate proportions using the ribbon method [46]. Provenance sensitive mineral ratios were also determined via the ribbon

counting method using a 100-grain count. Heavy mineral data and provenance-sensitive ratios are presented in Table 3.

Table 2. Petrographic results of Taimyr samples.

Sample	Formation	Qm	Qp	P	K	Lv	Ls
T99-26	Unnamed	213	29	1	43	0	0
T99-32	Unnamed	196	25	1	69	0	0
RAS98-8	Byrrangskaya	184	40	4	0	0	52
RAS98-9	Byrrangskaya	135	32	10	10	1	33
RAS98-32	Byrrangskaya	84	46	21	15	5	38
RAS98-23	Turozovskya	117	64	31	6	3	44
VP10-12	Baykurskaya	195	65	45	20	90	70
VP10-14	Sokolinskaya	230	55	75	40	25	40
VP10-25	Turozovskya	295	60	60	10	30	10

Notes: Qm = monocrystalline quartz (>0.0625 mm); Qp = polycrystalline quartz; total quartzose grains; P = plagioclase grains; K = K-feldspar grains; Lv = volcanic/metavolcanic lithic fragments; Ls = sedimentary/metasedimentary lithic fragments.

3.3. Detrital Zircon Geochronology

Detrital zircons from five samples (VP10-12, VP10-14, and VP10-25, RAS98-8 and RAS99-26) were dated using laser ablation inductively-coupled plasma mass spectrometry (LA-ICP-MS). Zircons were separated from about 2 kg of sample using conventional water table and heavy liquid mineral separation techniques. Around 300 grains were handpicked onto double-sided tape, cast into an epoxy resin disk and polished. Scanning electron microscope (SEM) and cathodoluminescence (CL) images were prepared for all grains using a Hitachi SEM at the Swedish Museum of Natural History or a JEOL JSM-820 SEM at the Department of Earth Sciences, University of Cambridge, to observe the textures of zircons. For samples from near the eastern coast in southern Taimyr, the LA-ICP-MS zircon U-Pb analyses were conducted using a Thermo X-series II quadrupole mass spectrometer equipped with a New Wave NWR193 excimer laser at the Petrotectonics Analytical Facility, Department of Geological Sciences, Stockholm University. Pb/U calibration was performed relative to the zircon standard Plešovice [47] and FC-5z [48]; the beam diameter was 25 μm. The raw data were processed using an Iolite [49,50] with the integral Vizual Age DRS (data reduction scheme) routine of Petrus and Kamber [51]. For samples RAS98-8 and RAS99-26, the LA-ICP-MS zircon U-Pb analyses were performed using a New Wave 213 aperture imaged frequency quintupled laser ablation system coupled to an Agilent 750a quadrupole-based ICP-MS. Real-time data were processed using GLITTER. Pb/U calibration was performed relative to the Plešovice zircon standard [47] and National Institute of Standards and Technology (NIST) 612 silicate glass [52]. All concordia diagrams and probability density distribution plots were made using ISOPLOT/Ex 4.15 [53]. All errors are reported at the 2-sigma level.

Table 3. Heavy mineral assemblage and ratios of Taimyr samples.

Samples	**T99-26**	**T99-32**	**RAS98-8**	**RAS98-9**	**RAS98-23**	**VP10-12**	**VP10-14**	**VP10-25**
Formation	**Unnamed**	**Unnamed**	**Byrrangskaya**	**Byrrangskaya**	**Turozovskya**	**Baykurskaya**	**Sokolinskaya**	**Turozovskya**
Heavy mineral assemblages								
apatite	1	9	41	159	163	79	99	58
tourmaline	14	36	162	138	49	61	39	25
zircon	52	64	200	28	114	30	192	109
garnet	45	39	7	3	7	50	15	7
hornblende	0	0	0	0	1	19	8	8
rutile	7	16	23	6	11	18	17	36
chloritoid	0	0	24	0	0	23	13	7
monazite	0	2	0	0	5	12	21	10
staurolite	347	256	0	0	0	16	7	8
epidote	4	10	0	7	0	44	29	9
titanite	1	5	10	0	12	4	19	6
sillimanite	0	0	0	2	1	0	3	2
chrome spinel	0	0	6	0	7	0	0	0
Total	471	437	473	343	370	356	462	285
Heavy mineral ratios								
apatite-tourmaline (ATi)	27	21	20	54	77	54	72	70
total	44	95	203	297	214	100	200	83
garnet-zircon (GZi)	49	43	3	5	6	63	7	6
total	238	231	207	86	121	80	207	116
monazite-zircon (MZi)	0	2	0	0	4	26	10	6
total	122	133	200	82	119	47	200	100

4. Results

4.1. Petrography

The petrographic results of nine samples are presented in Table 2 and Figure 4. For samples from the vicinity of Lake Taimyr, the Turozovskya Formation sample (RAS98-23) is a feldspathic litharenite. Byrrangskaya Formation samples (RAS98-8, RAS98-9 and RAS98-32) are sublitharenite and feldspathic litharenite (Figure 4a). Samples are dominated by monocrystalline quartz (65%–82%), showing variable degrees of undulosity. This mineral texture is typical for plutonic rocks (e.g., [54]). Samples plot within the recycled orogenic field and represent quartzite and transitional recycled orogen detritus (Figure 4b,c).

Figure 4. (**a**) QtFL (Qt = Qm + Qp, F = total feldspar grains, L = total lithic fragments,) sandstone classification plot of Taimyr samples (after Folk [55]); (**b**) QtFL and (**c**) QmFLt (Lt = L + Qp) provenance discrimination diagrams (after Dickinson *et al*. [56]).

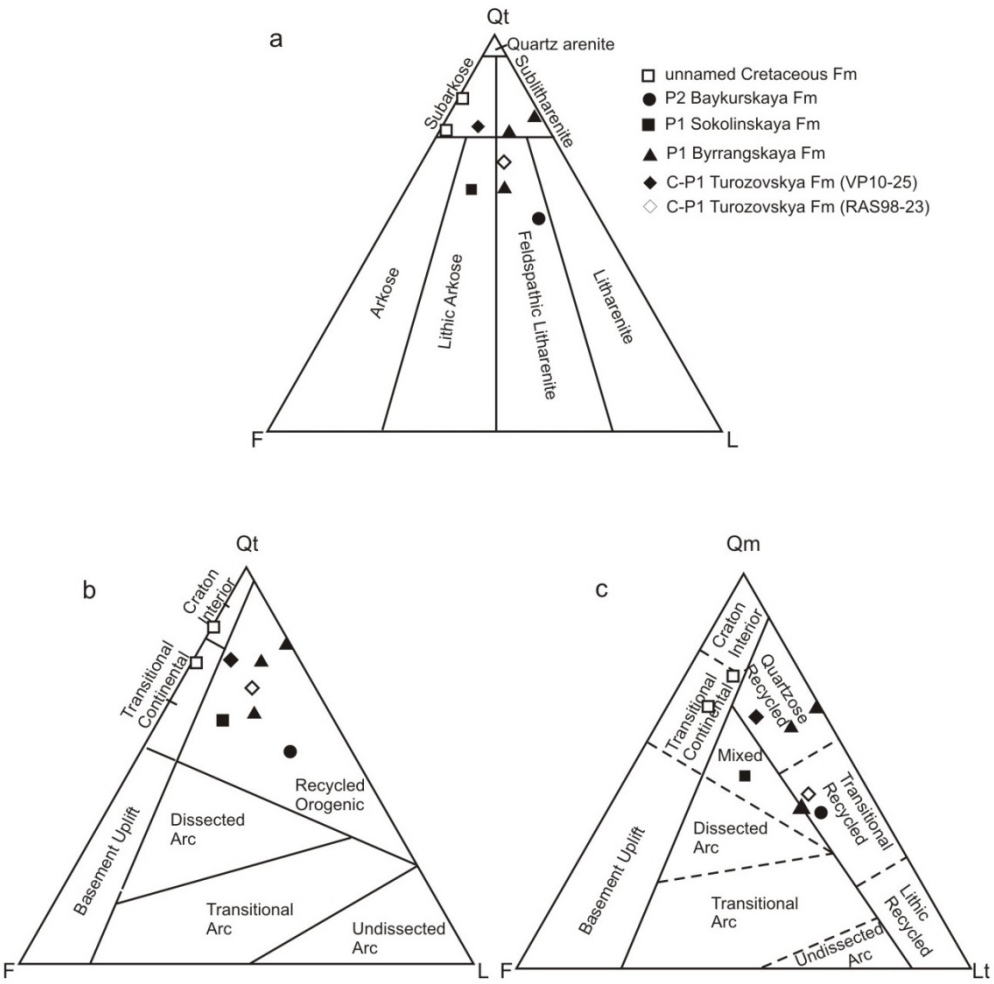

Samples from the eastern part of southern Taimyr, (the Turozovskya Formation sample VP10-25, the Sokolinskaya Formation sample VP10-14 and the Baykurskaya Formation sample VP10-12) are represented by subarkose, lithic arkose and feldspathic litharenite, respectively (Figure 4). They record decreasing sediment maturity through time. The Turozovskya Formation sample (VP10-25) shows

relatively high monocrystalline quartz (62%) and low polycrystalline quartz (5%), while the Permian samples (VP10-14 and VP10-12) contain less monocrystalline quartz (35%–38%) and increased polycrystalline quartz (15%–16%); this may reflect more detritus from metamorphic rocks in the Permian material. Microcline is present in all samples and provides evidence of a slowly cooled plutonic source. Recrystallization of quartz occurs in the late Permian Baykurskaya sample, indicating a distinct source compared to the pre-late Permian samples. The three samples plot within the "recycled orogenic" field. The Turozovskya Formation sample (VP10-25) represents a recycled quartzite source, while the Sokolinskaya Formation sample (VP10-14) plots within the mixed field and the Baykurskaya sample (VP10-12) represents a "transitional recycled orogen" source (Figure 4b,c).

The early Cretaceous samples show markedly different characteristics to the unconformably underlying Paleozoic samples. The Cretaceous samples are very coarse-grained and unconsolidated, whereas the Paleozoic samples are fine to medium-grained and strongly compacted and lithified. The Mesozoic samples represent subarkoses (Figure 4a). The quartz grains are almost exclusively monocrystalline, non-undulose quartz (80%–82%), indicative of a plutonic source. The feldspar compositions for these samples are almost exclusively alkali feldspar (98%–99%), often microcline and indicative of a proximal source. Samples plot within the "transitional continental" and "craton interior" fields (Figure 4b,c).

4.2. Heavy Mineral Results

The results of heavy mineral analysis are shown in Table 3 and Figure 5. For samples from the eastern part of southern Taimyr, the Turozovskya Formation sample VP10-25 and the Sokolinskaya Formation sample VP10-14 show similarity in heavy mineral assemblage, dominated by zircon (38%), apatite (20%) and rutile (11%–13%). Apatite grains are broken and rounded, indicating long distance transport. The late Permian Baykurskaya sample (VP10-12) has a distinctly different heavy mineral assemblage, containing apatite (22%), tourmaline (17%), garnet (14%) and zircon (8%). The prominent increase in garnet suggests a metamorphic source. Some apatite grains are euhedral, suggesting an additional and more proximal source for this sample.

The Turozovskya Formation sample (RAS98-23) near Lake Taimyr contains an ultrastable heavy mineral assemblage, dominated by apatite (44%), zircon (31%) and tourmaline (13%) (Figure 5a). Apatite grains are broken and rounded, suggesting sedimentary recycling and long-range transport. The zircon population is mixed, showing mostly rounded, recycled grains and some perfectly euhedral magmatic grains. Tourmaline grains also show two populations, with a mixture of broken, rounded brown grains and euhedral green grains. The heavy mineral assemblage contains minor amounts of less stable minerals, including hornblende and titanite. Importantly, the sample also contains minor chrome spinel (2%), a mineral indicating sediment derivation involving an ultramafic source. Early Permian Byrrangskaya Formation samples (RAS98-8 and RAS98-9) also contain stable heavy mineral assemblages, dominated by apatite (9% to 46%), zircon (8% to 42%) and tourmaline (34% to 40%). In sample RAS98-8, which contains 9% apatite, the morphology is rounded and broken, as seen in sample RAS98-23. In sample RAS98-9, which contains 46% apatite, the morphology is euhedral, suggesting an additional, more proximal apatite source. Both samples show a mixture of zircon

morphologies, with rounded and euhedral grains. Sample RAS98-8 contains 5% chloritoid and 1% chrome spinel.

Figure 5. (**a**) Taimyr heavy mineral assemblages, showing the relative abundance of heavy mineral species; (**b**) heavy mineral ratios of Taimyr sandstones. Indices are: GZi = [garnet/(garnet + zircon)] × 100; MZi = [monazite/(monazite + zircon)] × 100; ATi = [apatite/(apatite + tourmaline)] × 100.

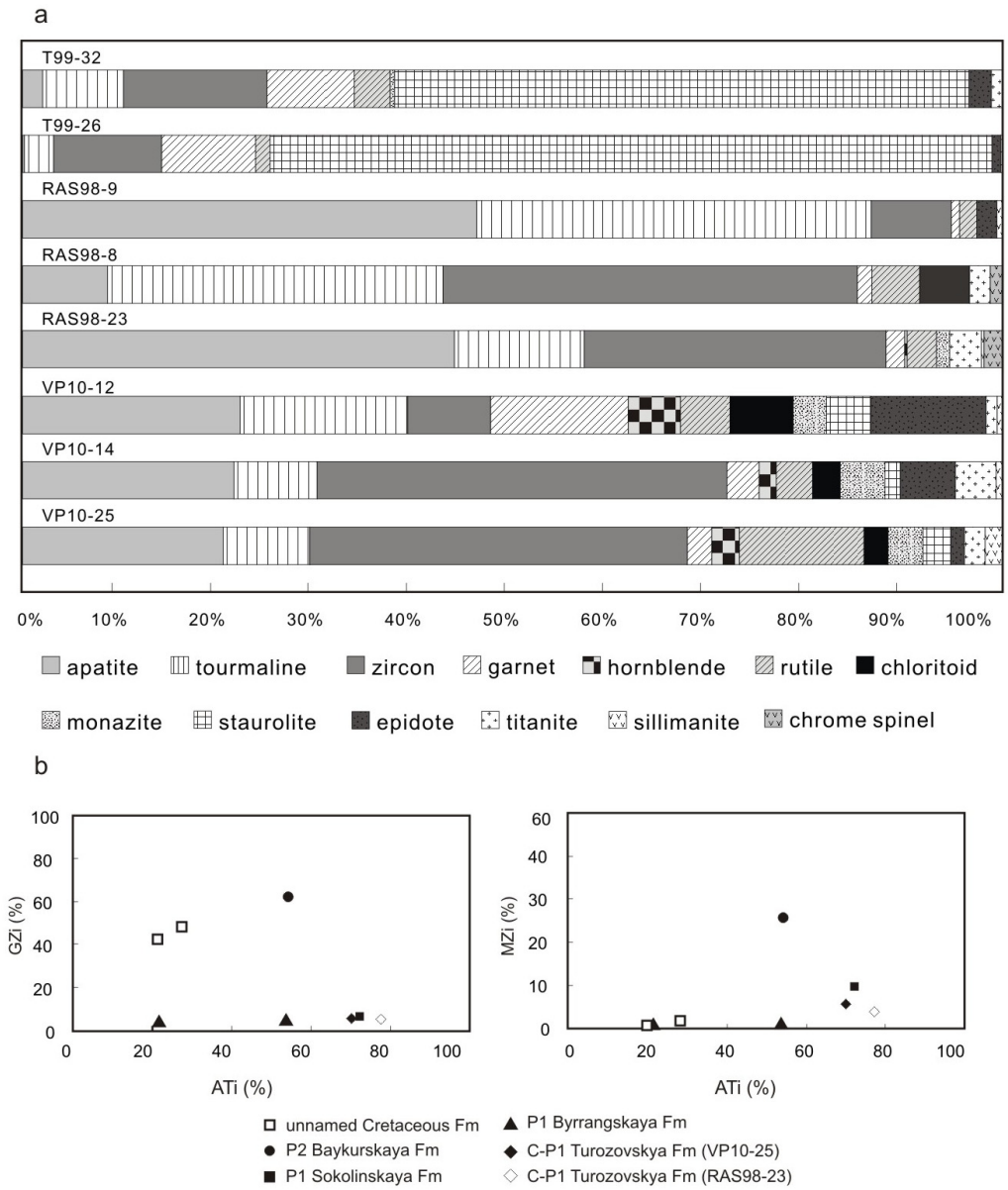

The early Cretaceous samples, T99-26 and T99-32, show very different heavy mineral assemblages in relation to the Permian samples and are dominated by the unstable mineral staurolite (59%–74%) (Figure 5a). Staurolite is a characteristic mineral of medium-grade metamorphic pelitic schists [57]. The samples also contain smaller amounts of zircon (11%–15%), garnet (9%–10%) and tourmaline (3%–8%). Most zircon grains show euhedral, doubly vergent, magmatic morphologies, although rounded grains are also present. Tourmaline grains are green and euhedral or rounded. Garnet grains in these samples are unetched.

Several other factors can affect the preservation of the heavy mineral assemblage, including weathering, transport, deposition and diagenesis [58]. To overcome such variations, the ratios of mineral abundance with similar hydraulic and diagenetic behavior can be used to determine provenance-related features of heavy mineral assemblages [59]. Some of our samples show variation of heavy mineral indices (Figure 5b), which are significant in the Permo-Carboniferous samples from the eastern part of southern Taimyr. In the Turozovskya Formation and Sokolinskaya Formation samples, the apatite-tourmaline (ATi) values exceed 70, and the garnet-zircon (GZi) and monazite-zircon (MZi) values are 3–7 and 4–10, respectively, whereas the Baykurskaya Formation sample has a lower ATi value (54) and higher GZi and MZi values (GZi = 63; MZi = 26). For samples from near Lake Taimyr, the Turozovskya Formation and Byrrangskaya Formation samples also present low GZi (3–6) and extremely low MZi (0–4) values. The variable ATi values (20–54) in two Byrrangskaya Formation samples, however, may be due to localized intrastratal dissolution [57,58]. The Cretaceous sample has low ATi values (21–27), extremely low MZi values (0–2) and medium GZi values (43–49).

4.3. Zircon Geochronology Results

Sample locations and analytical results for detrital zircon U-Pb dating are presented in Supplementary materials. For analyses, <1.0 Ga, $^{206}Pb/^{238}U$ ages are used, and $^{206}Pb/^{207}Pb$ ages are used for analyses >1.0 Ga. This is due to the better precision associated with the $^{206}Pb/^{238}U$ ages of "young" zircons, while for "older" zircons, the $^{206}Pb/^{207}Pb$ ages have more reliable uncertainties [60]. Analyses more than 10% discordant or with large errors (>10%) are excluded from the final data synthesis. CL images are presented in Figure 6. Relative probability plots for all samples (Figure 7), as well as for the younger (<1.0 Ga) components (Figure 8) are shown. We cite the peak ages, but it should be emphasized that each peak age also has an error of *ca.* ±15 Ma, and therefore, each peak age, in fact, represents an age range. The samples are compared using a cumulative age probability plot [61] (Figure 9).

Figure 6. Cathodoluminescence images of representative zircons from Taimyr samples. Analytical spots are indicated by circles.

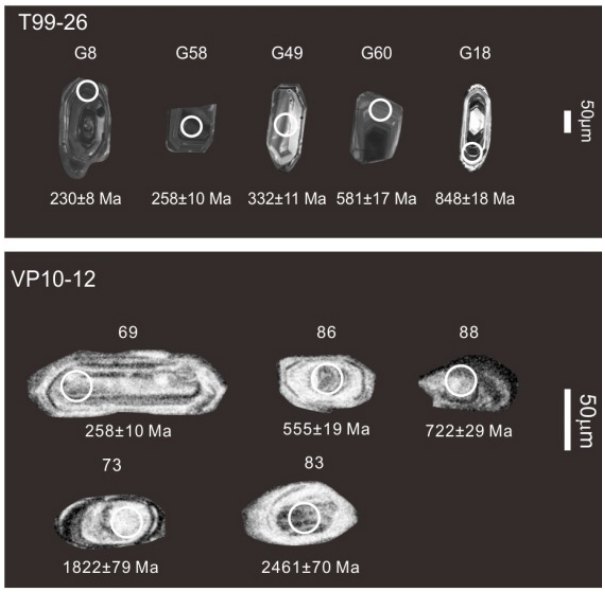

Figure 6. *Cont.*

Figure 7. Relative probability diagrams (with histograms) of U-Pb detrital zircon ages from the Taimyr Peninsula. Note that the youngest dominant peak in each sample is used to determine the maximum depositional age and *n* = concordant analyses/total analyses.

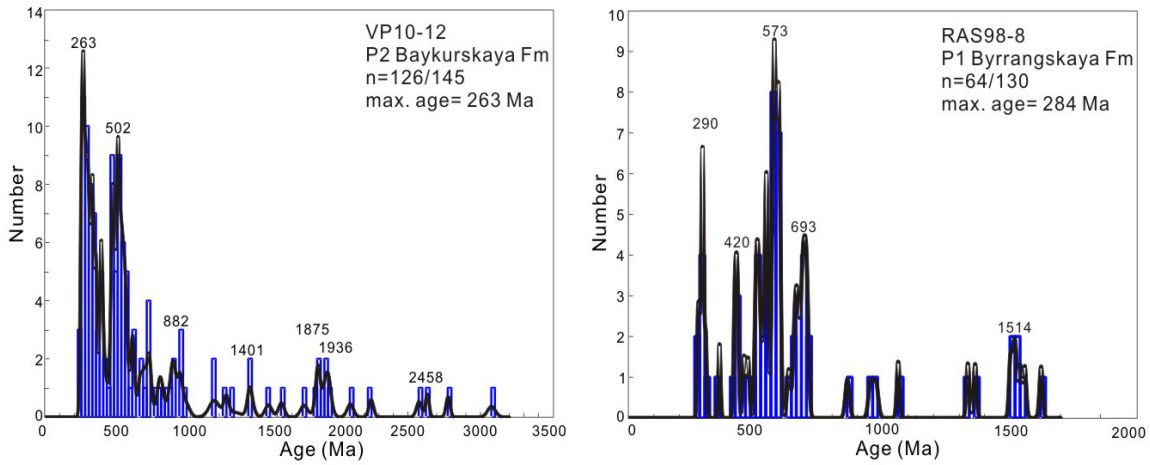

Figure 7. *Cont.*

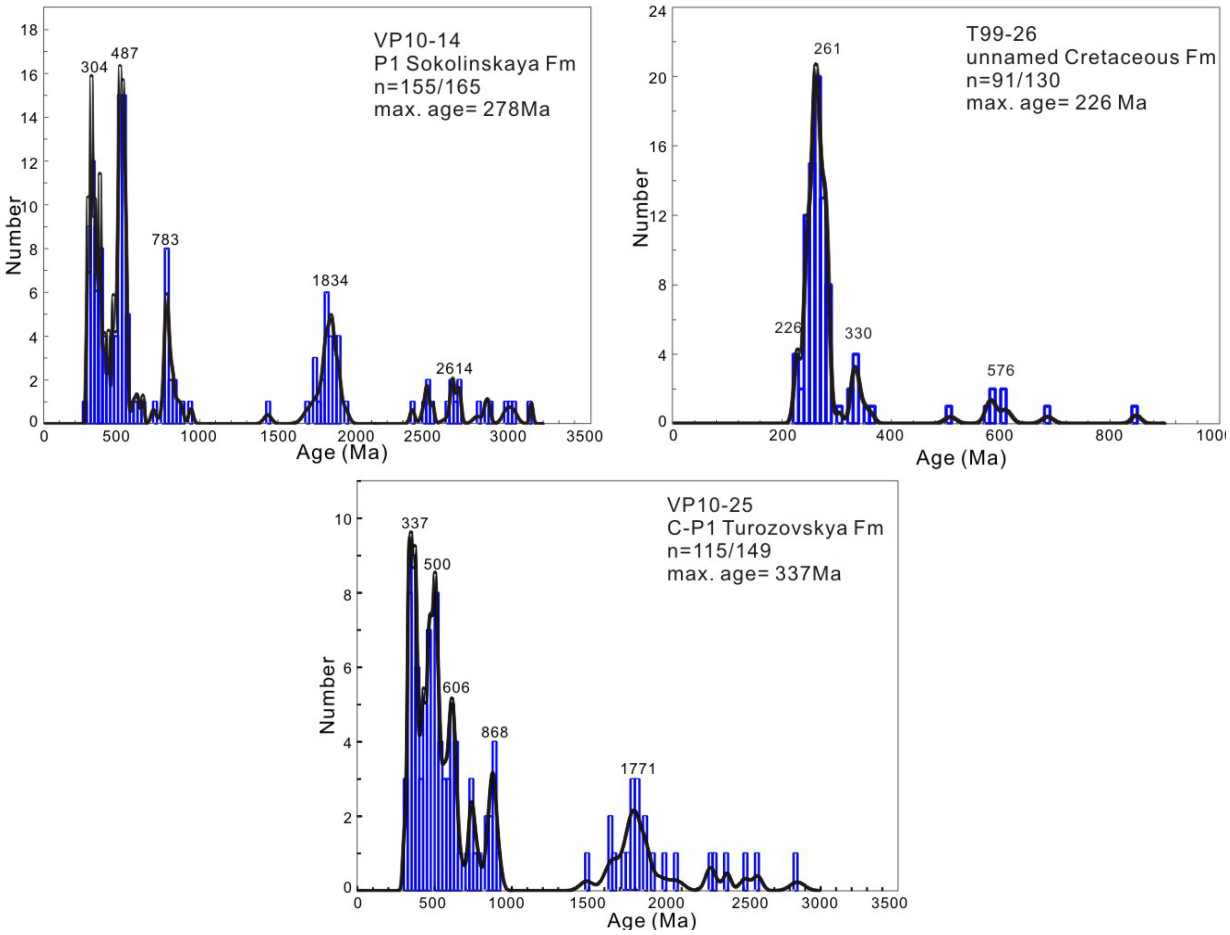

A total of 149 grains were analyzed for the Turozovskya Formation sample VP10-25, of which 115 are of acceptable quality. Most of the zircons are elongate and euhedral to subhedral with rounded terminations, and a few grains are round to elliptical (Figure 6). 26 analyses are Devonian to Carboniferous in age (415–301 Ma, with peaks at 369 Ma and 337 Ma). Another large age population is Cambrian to Ordovician, giving a significant peak at *ca*. 500 Ma, with an inflection at *ca.* 467 Ma and a smaller peak at 426 Ma. There are 33 Neoproterozoic ages (916–544 Ma, with peaks at *ca.* 868, 733 and 606 Ma) and a single Mesoproterozoic grain (1484 ± 86 Ma). A spread of Palaeoproterozoic ages (2395–1644 Ma) are present in this sample, with a peak at 1771 Ma. Three Archean ages also present, with ages of 2511, 2593 and 2849 Ma.

In total, 130 grains were analyzed from the Byrrangskaya Formation sample RAS98-8, of which only 64 analyses are within 10% of discordance. Of these, there are six early-Permian ages (295–273 Ma) peaking at 290 Ma (Figures 7 and 8), two Carboniferous grains (358 and 304 Ma) and four Silurian grains with a peak at 420 Ma. There are 13 latest Neoproterozoic–Ordovician grains (545–455 Ma, with peaks at 541 and 507 Ma). Twenty-seven grains of the ages are Neoproterozoic (703–566 Ma, with peaks at 693, 660, 589 and 573 Ma). There are nine Palaeoproterozoic to Mesoproterozoic ages (1622–1060 Ma). The morphology and internal structure of crystals range from rounded to euhedral, with many fragments (Figure 6). The youngest grains in the sample are Permian and show euhedral, magmatic morphology (e.g., G82 and G18 in Figure 6) [62], indicating a proximal source.

Figure 8. Close-up of Phanerozoic-Neoproterozoic relative probability diagrams (with histograms) of U-Pb detrital zircon ages from the Taimyr Peninsula. Green bars represent the age ranges discussed in this paper.

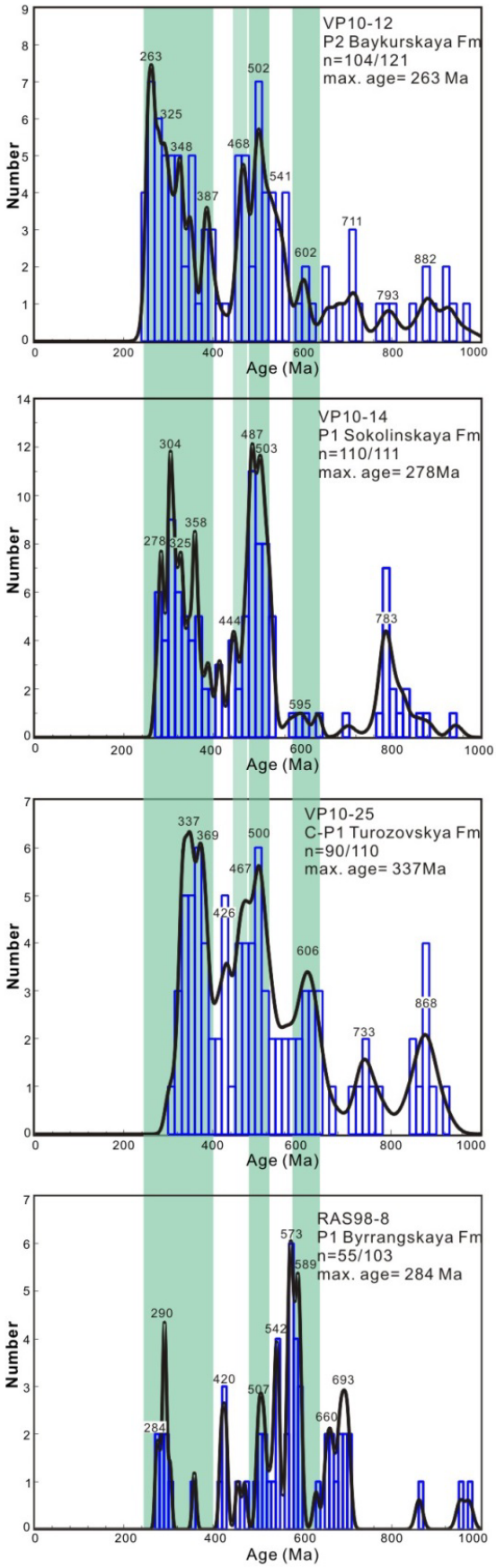

A total of 165 analyses were obtained from the Sokolinskaya Formation sample VP10-14, of which 155 are of acceptable quality. The morphology and internal texture of representative grains are seen via CL images (Figure 6). Its zircons are variably rounded to euhedral, with a lot of fragmental grains. There are 34 Carboniferous to Permian ages (359–271 Ma, with peaks at 358, 325, 304 and 278 Ma). The detrital age population contains abundant Cambrian to Ordovician grains with peaks at 487 and 503 Ma. There are 65 Precambrian ages, which are characterized by: (1) six Neoarchean ages (peak at *ca.* 2614 Ma) and six Mesoarchean ages, including two ages over 3000 Ma; (2) Palaeoproterozoic detritus ranging between 1600 and 2500 Ma with a large peak at *ca.* 1834 Ma and a small peak at 2448 Ma; (3) detritus with Neoproterozoic ages between 541 and 943 Ma, with a peak at *ca.* 783 Ma. Only a single Mesoproterozoic grain with an age of 1434 ± 48 Ma is present.

In total of 145 grains of Baykurskaya Formation sample VP10-12 were analyzed, of which 126 yielded ages within 10% of discordance. The sample has a wide spread in zircon ages (Figure 7). The dominant probability peak occurs at 263 Ma; 24 grains analyzed (299–242 Ma) contribute to this peak, and the corresponding zircons are euhedral and unaltered. There are 17 Carboniferous ages (357–300 Ma, with peaks at 348 and 325 Ma) and eight Devonian ages (411–374 Ma, with a peak at 387 Ma). The sample also has a large portion of zircons within the age range of 564–429 Ma, defining the main peak at 502 Ma with a shoulder at 541 Ma (Figure 8). There are 22 Neoproterozoic ages (973–591 Ma, with peaks at 882, 714 and 602 Ma), a spread of Mesoproterozoic ages (1539–1162 Ma) and 11 Palaeoproterozoic ages (2247–1628 Ma, with peaks at 1936 Ma and 1875 Ma). Four Archean grains (3076–2577 Ma) are present. Most old zircons mainly show rounded morphology, suggesting possible recycled sources (Figure 6).

Cretaceous sample T99-26, of which 91 yielded ages within 10% of discordance, is dominated by young, Permo-Triassic zircons. The Permo-Triassic peak consists of 69 grains (286–237 Ma, forming a peak at 261 Ma). A younger Triassic peak is defined by five grains (230–222 Ma) at 226 Ma. There are nine Carboniferous grains (362–305 Ma, forming a peak at 330 Ma) and eight Neoproterozoic-Cambrian grains (848–508 Ma, forming a peak of seven grains at 576 Ma) (Figure 7). The morphology and internal structure from CL images is seen in Figure 6. The Neoproterozoic-Cambrian grains and Carboniferous grains show rounded to near-euhedral morphology, mostly with complex magmatic zoning. The Permo-Triassic grains show predominantly euhedral morphology, with complex magmatic zoning.

5. Discussion

A Permo-Carboniferous compressional event, similar in age to Uralian orogeny, is well documented in Taimyr. The geologic affinities of Permo-Carboniferous sediments in Taimyr should help to constrain whether or not Uralian orogenesis extended to Taimyr. In addition, Early Cretaceous sedimentation is coeval with the opening of the Amerasian Basin and should provide information about Cretaceous tectonism in Taimyr. Consequently, the following discussion focuses on the provenance of and driving mechanisms for Permo-Carboniferous and Cretaceous sediment deposition in Taimyr.

5.1. Provenance of Permo-Carboniferous and Early Cretaceous Successions

The late Carboniferous to early Permian Turozovskya Formation and early Permian Byrrangskaya Formation samples from the vicinity of Lake Taimyr are characterized as feldspathic litharenite and

sublitharenite. The Turozovskya Formation, early Permian Sokolinskaya Formation and late Permian Baykurskaya Formation samples from the eastern part of southern Taimyr are classified as subarkose, lithic arkose and feldspathic litharenite, respectively—they record decreasing sediment maturity through time. All samples represent a recycled orogenic source (from Figure 4), suggesting these formations were produced through uplift and erosion of a rising collisional belt.

The heavy mineral assemblages of the Permo-Carboniferous samples are stable and dominated by mixed populations of apatite, zircon and tourmaline, with some chrome spinel in some samples (RAS98-8 and RAS98-23). The late Permian Baykurskaya Formation sample shows a dramatic decrease in zircon and an increase of garnet, suggesting an increased involvement of a metamorphic source. The increase in MZi ratio may be due to the input of syenitic granites corresponding to the syn- and post-tectonic syenite of northern Taimyr [59]. The similarities and variations among the heavy mineral ratio indices of these samples indicate that the sources for the late Carboniferous to early Permian and early Permian samples probably share a common provenance, whereas the late Permian sample has a distinctly different source.

The main characteristic of the detrital zircon age spectra for the four southern Taimyr Permo-Carboniferous samples is that they all preserve significant Uralian age grains (337–263 Ma), which are very close to their stratigraphic ages. The corresponding zircons are mostly euhedral and with magmatic textures, indicating relatively proximal first cycled magmatic sources and requires relatively fast erosion and transport of zircons from source to sink [63]. The later stage of Uralian orogenesis is characterized by magmatic activity varying from the late Devonian to mid/late Permian age [5,64–67]. Thus, the evidence suggests that the Uralian Orogen was a significant source during the deposition of southern Taimyr Permo-Carboniferous sedimentary successions. Likely source areas for this succession could be (i) the Uralian Orogen to the north or northwest of Taimyr; (ii) from the west-northwest (WNW), where the Uralian Orogen may be buried beneath the southern Kara Sea; (iii) from the Polar Urals, or some combination of the three. However, the proximal nature of the sediments probably favors a source closer than the Polar Urals.

A common age peak of *ca.* 500 Ma is present in these Permo-Carboniferous samples. Triassic sandstones from the New Siberian Islands and Chukotka belonging to the paleo-Taimyr river system also contain significant Cambro-Ordovician grains [5]. This age population is similar to the 500–505 Ma peak reported by Pease and Scott [24] for Cambro-Ordovician sediments from Novaya Zemlya, which they relate to the latest Timanian accretionary event. Geophysical evidence suggests that the Timanian Orogen extends beyond southern Novaya Zemlya and mimics its arcuate shape [68]. Thus, the presence of the *ca.* 500 Ma age peak may reflect recycling of Timanian input in the region. The Timanides are an accretionary orogen along the eastern and northeastern margin of Baltica of late Neoproterozoic age (see [25] and references therein), and Timanian detrital zircon ages represent a "fingerprint" for establishing a Baltica affinity. Therefore, the presence of Timanian ages in Permo-Carboniferous clastics indicates Baltica input to sediments of southern Taimyr (Siberia) during the late Paleozoic. The Middle Ordovician to Middle Devonian ages present in all these samples may represent ultimate derivation from the Caledonian Orogen or pre-Uralian magmatism. The Palaeoproterozoic and Archean detrital zircons are likely derived from older basement, perhaps from central Taimyr.

Comparing the youngest Baykurskaya Formation sample (VP10-12) to the older samples, a striking difference is the distinct occurrence of 1000–1500 Ma ages in the younger sample (VP10-12). These

Mesoproterozoic ages are also reported by Lorenz *et al.* [69] from Paleozoic successions on Severnaya Zemlya and are correlative with the Mesoproterozoic accreted domains of the Baltic Shield. Detrital zircons with such ages are present in Neoproterozoic to early Paleozoic strata deposited adjacent to the Baltica shield [70], but not in sediments on Siberia. Therefore, Baltica is a more probable source for zircon grains with 1000–1500 Ma ages. The Palaeoproterozoic ages (2247–1628 Ma, with peaks at 1936 and 1875 Ma) may also reflect input from Baltica, since magmatism was significant in Baltica from 1.8 to 2.3 Ga [71].

Neoproterozoic ages (690–730 Ma) in the Baykurskaya Formation sample may correspond to intrusive and extrusive island arc magmatism recorded in northern Taimyr (700 Ma) [72] and/or the ophiolite belt in central Taimyr (730–750 Ma) [37]. The late Permian Baykurskaya Formation sample has significant zircon grains in the age range around *ca.* 541 Ma, which is typical of granitic magmatism in the Timanides (see [25] and references therein, [73]). Baltica would have collided with southern and central Taimyr during Uralian orogeny [10,20,39,74], and it is highly likely that the early Paleozoic succession in northern Taimyr with Baltica affinity preserved Timanide-derived detritus. The presence of late Vendian to early Cambrian zircon ages, plus the late Paleozoic ages in the late Permian Baykurskaya formation sample suggests that Timanian-aged material was later recycled during the late Paleozoic Uralian orogeny and deposited in southern Taimyr.

The early Permian Byrrangskaya Formation sample collected from the vicinity of Taimyr Lake is about 350 km east of the other sample locations. There are no Palaeoproterozoic to Archean zircons in this sandstone, which may be due to a real change of provenance, the small dataset (n = 55) or a different sediment pathway between the two sampling locations, resulting in the differences between them.

During Triassic time, the Taimyr Peninsula underwent dextral transpression with associated uplift and erosion [20,21,31]. There are no early Triassic-Pliensbachian sediments preserved on the Taimyr Peninsula or Severnaya Zemlya. Toarcian sediments unconformably overlie deformed Neoproterozoic-Permian strata. The early Cretaceous samples are subarkoses and plot within the "continental" fields on QtFL and QmFLt diagrams (Figure 4). These coarse-grained samples are dominated by non-undulose monocrystalline quartz grains, representative of a plutonic quartz source. Feldspar compositions are predominantly alkali feldspar, also suggesting a plutonic source. The heavy mineral fraction analyzed is from a different size fraction (fine-grained sand *vs.* coarse-grained sand), such that the grains may be providing different sediment provenance information. Nevertheless, the early Cretaceous samples are unconsolidated and show an immature heavy mineral assemblage, dominated by staurolite, clearly indicating a low-grade metamorphic source. Zircon and tourmaline grains are euhedral, suggesting local derivation. The euhedral and immature character of the mineral assemblage suggests a proximal source for this sediment.

Zircon in the Cretaceous samples is dominated by a robust Permo-Triassic (286–237 Ma) peak at 261 Ma. These magmatic, euhedral zircons may reflect Siberian trap-related zircon-bearing magmatism on Taimyr and nearby islands. Known sources for zircons of this age include gabbros on the New Siberian Islands [75], syenites and dolerites of northern Taimyr and nearby islands in the eastern Barents Sea [76]. This sample contains some older zircon grains: Neoproterozoic–Cambrian ages (610–508 Ma) correspond with magmatic events in the Timanian Orogen, and Carboniferous grains (362–328 Ma) likely correspond to magmatism within the Uralian Orogen.

5.2. Uralian Orogeny vs. *Mesozoic Folding and Thrusting*

The petrographic and heavy mineral results discussed above indicate that a different source was involved in the deposition of late Permian sediments compared with the older strata. This inference is also supported by the detrital zircon results. The Kolmogorov-Smirnov (K-S) test [77] was applied to examine the possibility of significant differences between zircon age populations of different samples. The confidence level is 95%, and when the *p*-value is larger than 0.05, the zircon populations are considered to be similar. The K-S test suggests strong correlation between the Turozovskya Formation sample (VP10-25) and the Sokolinskaya Formation sample (VP10-14) (*p*-value = 0.309) and no correlation between the Baykurskaya Formation sample (VP10-12) with either of the other two samples (Figure 9). The K-S test *p*-value for the Byrrangskaya Formation sample and the Turozovskya Formation sample is 0.082, indicating a possible, but weak, correlation between these two formations.

Figure 9. (**a**) Cumulative probability plots of the zircon age data for Taimyr late Paleozoic and Mesozoic samples. The grey region represents Jurassic-Cretaceous detrital zircon ages from Miller *et al.* [32]; (**b**) *p*-values resulting from K-S test.

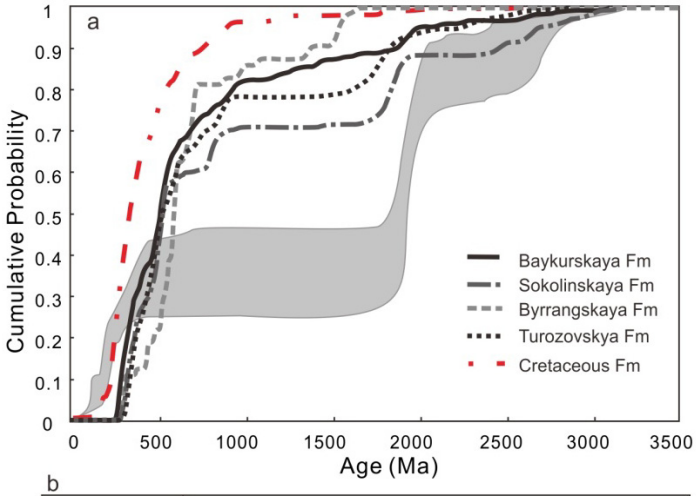

b

	K-S P-values using error in the CDF			
	P_2bk fm	P_1sk fm	C_3-P_1tr fm	P_1br fm
P_2bk fm		0.036	0.010	0.005
P_1sk fm	0.036		**0.309**	0.001
T_2-P_1tr fm	0.010	**0.309**		**0.082**
P_1br fm	0.005	0.001	**0.082**	

Both northern Taimyr and Severnaya Zemlya are related to Baltica [16,24,78], and its location is close to Novaya Zemlya [9], the curved shape of which may represent a natural embayment of Baltica's Paleozoic margin [15], possibly formed during Timanian accretion [68]. On the basis of seismic data, Malyshev *et al.* [79] suggest that the North Siberia Arch is a link between Novaya Zemlya and northern Taimyr and was part of the Paleozoic continental margin; Paleozoic deformation extends across the North Siberia Arch in the Carboniferous, reaching north of northern Taimyr (Figure 1a). This suggests that the Uralian Orogen continues northward across the Kara Sea to Taimyr.

The Permo-Carboniferous successions all record contemporaneous late Paleozoic unroofing and have younging age peaks (337–263 Ma) consistent with their relative stratigraphic positions; we

interpret this to represent the northern continuation of Uralian orogenesis in Taimyr. All Paleozoic samples contain syn-sedimentary zircon grains and older input consistent with Baltica and/or central Taimyr, indicating a foreland basin setting [80]. Given that the Baykurskaya Formation sandstone is less mature, it should have a more proximal source than the older samples. The syn- and post-collisional granitic intrusions with ages of 300–265 Ma in northern Taimyr [39–41] represent Uralian orogenesis in this area. These ages are well documented in the Baykurskaya Formation sample, indicating that erosion during late Paleozoic uplift associated with Uralian orogenesis in northern Taimyr provided significant input to Baykurskaya Formation clastic sedimentation. Thus, it is likely that the syn-tectonic zircons in the pre-late Permian deposits derive from the Uralian Orogen to the WNW, while the late Permian sediments have a Uralian source from northern Taimyr. In this case, the younging detrital zircon ages in the Permo-Carboniferous successions are consistent with diachronous Uralian orogenesis [13,64].

Furthermore, zircon ages associated with Baltica basement (1.0–1.5 Ma) and typical Timanian ages (550 Ma) reflect a Baltica fingerprint that is only present in late Permian deposits. Therefore, we infer that northern Taimyr and Severnaya Zemlya, as a part of Baltica, collided with the Siberian margin (central Taimyr) between the early and late Permian. This supports the two-phase deformation model proposed by Inger *et al.* [20], in which the early phase is equated with Permo-Carboniferous Uralian deformation and, later, followed by Triassic dextral transcurrent deformation.

5.3. Tectonic Setting of Taimyr in the Cretaceous

Miller *et al.* [32] report detrital zircon ages for syn-orogenic Jurassic to Cretaceous foreland basin deposits from the New Siberia Islands and Chukotka, pointing out that they likely derived from the Mesozoic Verkhoyansk Fold Belt (VFB). The VFB is interpreted to result from the closure of the Angayucham-south Anyui Ocean just prior to the opening of the Amerasian Basin [70]. Their results document a distinct detrital signature containing contemporary orogenic zircons and abundant Precambrian zircons. This is quite different from our results (Figure 9), in which Jurassic to Cretaceous ages are absent and only a few Neoproterozoic ages occur. Therefore, the early Cretaceous deposits in northern Taimyr seem unrelated to the deformation associated with the Mesozoic VFB, and thus, the detritus shed from this fold belt did not extend to northern Taimyr.

The absence of zircons with syn-depositional ages in sediments is typical of rift basin and passive margin detritus [80] and our detrital zircon data and sandstone compositions are consistent with an extensional setting, such as a rift or passive margin setting. Grantz *et al.* [81] argue for a strike-slip Eurasian margin in the counterclockwise rotational opening model for the Amerasian Basin, which may support a transtensionsal setting for northern Taimyr during the early Cretaceous; however, it is difficult to envision regional-scale Cretaceous deposition via this mechanism. Miller *et al.* [70] suggest the Siberia rift extended into the paleo-Pacific margin during Triassic to Cretaceous time in the bi-rotational model [82,83]. Taimyr is to the north of the inferred Siberia rift in this scenario; however, a rift-related deposition in northern Taimyr is unlikely. Consequently, a passive margin setting for Taimyr in Cretaceous time is indicated and not accounted for in existing models for the development of the Amerasian Basin.

6. Conclusions

Permo-Carboniferous sedimentary rocks of southern Taimyr preserve a mixed provenance of recycled and first cycle detritus, sourced from metamorphic and igneous lithologies. The decreasing maturity of the sediment and younging detrital zircon age peaks with time is consistent with the diachronous Uralian Orogen, younging from south to north, extending into the Taimyr region. The late Carboniferous to early Permian Turozovskya Formation and the early Permian Sokolinskaya Formation show little evidence for derivation from northern Taimyr and are more consistent with Uralian sources to the WNW, which may currently lie beneath the Kara Sea. The late Permian Baykurskaya Formation records local derivation from northern Taimyr with a large clastic component inferred to be derived from Baltica. The data suggest that:

1. The Permo-Carboniferous successions were deposited in a foreland basin of the Uralian Orogen, consistent with the northwards continuation of the Urals into Taimyr. The final collision between Baltica and Siberia in the latest stage of Uralian orogenesis occurred in the late Permian, as recorded by the dramatic change in provenance associated with late Permian sandstone.
2. Early Cretaceous sediments in northern Taimyr are proximal and have significant input from Siberian trap-related magmatism found in and near the Taimyr Peninsula. Cretaceous sediment provenance suggests deposition in a rift or passive margin setting and is unrelated to Jura-Cretaceous crustal shortening and arc collision associated with the Verkhoyansk Fold Belt. Consequently, a Cretaceous passive margin setting seems likely.

Acknowledgements

We are grateful for logistical support from the Swedish Polar Research Secretariat, the Swedish Research Council (funding to V. Pease) and the YMER-80 fund (to X. Zhang). We thank A. Morton for guidance on heavy mineral analysis. Thanks also to E. Arnold for helpful suggestions on an earlier version of this manuscript, to C. Wohlgemuth-Ueberwasser at Stockholm University, P. Persson and K. Lindén at the Natural History Museum and S. Lundqvist at SGU for assistance with the laboratory work. Thanks to P. Möller at Lund University for collecting the Cretaceous samples. We thank S. Drachev and A. Wilner for constructive comments, which improved this paper. This is a CALE publication.

Conflict of Interest

The authors declare no conflict of interest.

References

1. Zonenshain, L.; Korinevsky, V.; Kazmin, V.; Pechersky, D.; Khain, V.; Matveenkov, V. Plate tectonic model of the South Urals development. *Tectonophysics* **1984**, *109*, 95–135.
2. Hamilton, W. The Uralides and the motion of the Russian and Siberian platforms. *Geol. Soc. Am. Bull.* **1970**, *81*, 2553–2576.

3. Brown, D.; Spadea, P.; Puchkov, V.; Alvarez-Marron, J.; Herrington, R.; Willner, A.P.; Hetzel, R.; Gorozhanina, Y.; Juhlin, C. Arc–continent collision in the Southern Urals. *Earth Sci. Rev.* **2006**, *79*, 261–287.
4. Shipilov, E.; Vernikovsky, V. The Svalbard–Kara plates junction: Structure and geodynamic history. *Russ. Geol. Geophys.* **2010**, *51*, 58–71.
5. Miller, E.L.; Soloviev, A.V.; Prokopiev, A.V.; Toro, J.; Harris, D.; Kuzmichev, A.B.; Gehrels, G.E. Triassic river systems and the paleo-Pacific margin of northwestern Pangea. *Gondwana Res.* **2012**, *23*, 1631–1645.
6. Nikishin, A.; Ziegler, P.; Stephenson, R.; Cloetingh, S.; Furne, A.; Fokin, P.; Ershov, A.; Bolotov, S.; Korotaev, M.; Alekseev, A. Late Precambrian to Triassic history of the East European Craton: Dynamics of sedimentary basin evolution. *Tectonophysics* **1996**, *268*, 23–63.
7. Lawver, L.A.; Grantz, A.; Gahagan, L.M. Plate kinematic evolution of the present Arctic region since the Ordovician. *Geol. Soc. Am. Spec. Pap.* **2002**, *360*, 333–358.
8. Drachev, S.S. Tectonic setting, structure and petroleum geology of the Siberian Arctic offshore sedimentary basins. *Geol. Soc. Lond. Mem.* **2011**, *35*, 369–394.
9. Pease, V. Eurasian orogens and Arctic tectonics: An overview. *Geol. Soc. Lond. Mem.* **2011**, *35*, 311–324.
10. Otto, S.; Bailey, R. Tectonic evolution of the northern Ural Orogen. *J. Geol. Soc.* **1995**, *152*, 903–906.
11. Korago, E.A.; Kovaleva, G.N.; Lopatin, B.G.; Orgo, V.V. The precambrian rocks of Novaya Zemlya. *Geol. Soc. Lond. Mem.* **2004**, *30*, 135–143.
12. O'leary, N.; White, N.; Tull, S.; Bashilov, V.; Kuprin, V.; Natapov, L.; Macdonald, D. Evolution of the Timan–Pechora and south barents sea basins. *Geol. Mag.* **2004**, *141*, 141–160.
13. Puchkov, V. Tectonics of the Urals: Modern concepts. *Geotectonics* **1997**, *31*, 294–312.
14. Gee, D.G.; Bogolepova, O.K.; Lorenz, H. The Timanide, Caledonide and Uralide orogens in the Eurasian high Arctic, and relationships to the palaeo-continents Laurentia, Baltica and Siberia. *Geol. Soc. Lond. Mem.* **2006**, *32*, 507–520.
15. Scott, R.A.; Howard, J.P.; Guo, L.; Schekoldin, R.; Pease, V. Offset and curvature of the Novaya Zemlya fold-and-thrust belt, Arctic Russia. *Pet. Geol. Conf. Ser.* **2010**, *7*, 645–657.
16. Drachev, S.S.; Malyshev, N.A.; Nikishin, A.M. Tectonic history and petroleum geology of the Russian Arctic Shelves: An overview. *Pet. Geol. Conf. Ser.* **2010**, *7*, 591–619.
17. Sengör, A.; Natal'in, B.; Burtman, V. Evolution of the Altaid tectonic collage and Paleozoic crustal growth in Eurasia. *Nature* **1993**, *364*, 299–307.
18. International Bathymetric Chart of the Arctic Ocean (IBCAO) database Home Page. http://www.ngdc.noaa.gov/mgg/bathymetry/arctic/-arctic.html (accessed on 25 July 2013).
19. Bezzubtsev, V.; Malitch, N.; Markov, F.; Pogrebitsky Yu, E. *Geological Map of Mountainous Taimyr 1: 500,000, Ministry of Geology of the USSR* [in Russian]; Ministry of Geology of the Russian Federation (RSFSR), Krasnoyarskgeologia: Krasnoyarsk, Russian, 1983.
20. Inger, S.; Scott, R.; Golionko, B. Tectonic evolution of the Taimyr Peninsula, northern Russia: Implications for Arctic continental assembly. *J. Geol. Soc.* **1999**, *156*, 1069–1072.

21. Walderhaug, H.; Eide, E.; Scott, R.; Inger, S.; Golionko, E. Palaeomagnetism and $^{40}Ar/^{39}Ar$ geochronology from the South Taimyr igneous complex, Arctic Russia: A Middle–Late Triassic magmatic pulse after Siberian flood-basalt volcanism. *Geophys. J. Int.* **2005**, *163*, 501–517.
22. Lorenz, H.; Gee, D.G.; Whitehouse, M.J. New geochronological data on Palaeozoic igneous activity and deformation in the Severnaya Zemlya Archipelago, Russia, and implications for the development of the Eurasian Arctic margin. *Geol. Mag.* **2007**, *144*, 105–125.
23. Lorenz, H.; Männik, P.; Gee, D.; Proskurnin, V. Geology of the Severnaya Zemlya Archipelago and the North Kara Terrane in the Russian high Arctic. *Int. J. Earth Sci.* **2008**, *97*, 519–547.
24. Pease, V.; Scott, R.A. Crustal affinities in the Arctic Uralides, northern Russia: Significance of detrital zircon ages from Neoproterozoic and Palaeozoic sediments in Novaya Zemlya and Taimyr. *J. Geol. Soc.* **2009**, *166*, 517–527.
25. Gee, D.G.; Pease, V. *The Neoproterozoic Timanide Orogen of Eastern Baltica*; Geological Society Publishing House: London, UK, 2004.
26. Lorenz, H.; Gee, D.G.; Larionov, A.N.; Majka, J. The Grenville–Sveconorwegian orogen in the high Arctic. *Geol. Mag.* **2012**, *149*, 875–891.
27. Dobretsov, N.; Vernikovsky, V. Mantle plumes and their geologic manifestations. *Int. Geol. Rev.* **2001**, *43*, 771–787.
28. Reichow, M.K.; Pringle, M.; Al'Mukhamedov, A.; Allen, M.; Andreichev, V.; Buslov, M.; Davies, C.; Fedoseev, G.; Fitton, J.; Inger, S. The timing and extent of the eruption of the Siberian Traps large igneous province: Implications for the end-Permian environmental crisis. *Earth Planet. Sci. Lett.* **2009**, *277*, 9–20.
29. Nikishin, A.; Ziegler, P.; Abbott, D.; Brunet, M.-F.; Cloetingh, S. Permo–Triassic intraplate magmatism and rifting in Eurasia: Implications for mantle plumes and mantle dynamics. *Tectonophysics* **2002**, *351*, 3–39.
30. Saunders, A.D.; England, R.W.; Reichow, M.K.; White, R.V. A mantle plume origin for the Siberian traps: uplift and extension in the West Siberian Basin, Russia. *Lithos* **2005**, *79*, 407–424.
31. Torsvik, T.H.; Andersen, T.B. The Taimyr fold belt, Arctic Siberia: Timing of prefold remagnetisation and regional tectonics. *Tectonophysics* **2002**, *352*, 335–348.
32. Miller, E.L.; Soloviev, A.; Kuzmichev, A.; Gehrels, G.; Toro, J.; Tuchkova, M. Jurassic and Cretaceous foreland basin deposits of the Russian Arctic: Separated by birth of the Makarov Basin? *Norw. J. Geol.* **2008**, *88*, 201–226.
33. Vernikovsky, V. The geodynamic evolution of the Taimyr folded area. *Geol. Pac. Ocean* **1996**, *12*, 691–704.
34. Bezzubtsev, V.; Zalyaleyev, R.; Sakovich, A. *Geological Map of Mountainous Taimyr 1: 500,000: Explanatory Notes* [in Russian]; Ministry of Geology of the Russian Federation (RSFSR), Krasnoyarskgeologia: Krasnoyarsk, Russian, 1986.
35. Zonenshain, L.; Kuzmin, M.; Natapov, L. *Geology of the USSR: A Plate-Tectonic Synthesis (American Geophysical Union, Geodynamics Series), 21*; American Geophysical Union: Washington, DC, USA, 1990.
36. Uflyand, A.; Natapov, L.; Lopatin, V.; Chernov, D. On the Taimyr tectonic nature. *Geotectonics* **1991**, *6*, 76–79.

37. Vernikovsky, V.; Vernikovskaya, A.; Pease, V.; Gee, D. Neoproterozoic orogeny along the margins of Siberia. *Geol. Soc. Lond. Mem.* **2004**, *30*, 233–248.
38. Pease, V.; Gee, D.G.; Vernikovsky, V.; Vernikovskaya, A.; Kireev, S. Geochronological evidence for late-Grenvillian magmatic and metamorphic events in central Taimyr, northern Siberia. *Terra Nova* **2001**, *13*, 270–280.
39. Vernikovsky, V.; Neimark, L.; Ponomarchuk, V.; Vernikovskaya, A.; Kireev, A.; Kuz'Min, D. Geochemistry and age of collision granitoides and metamorphites of the Kara microcontinent (Northern Taimyr). *Russ. Geol. Geophys.* **1995**, *36*, 46–60.
40. Vernikovsky, V.; Sal'nikova, E.; Kotov, A.; Ponomarchuk, V.; Kovach, V.; Travin, A.; Yakovleva, C.; Berezjnava, N. Age of post-collisional granitoids of Northern Taimyr: U-Pb, Sm-Nd, Rb-Sr, and Ar-Ar dat. *Dokl. RAN* **1998**, *363*, 375–378.
41. Pease, V. Department of Geological Sciences, Stockholm University, Stockholm, Sweden, unpublished work.
42. Natapov, L.M.; Paraketsov, K.V.; Kulikova, L.I.; Kononov, M.N. Jurassic-Cretaceous Tectonostratigraphy of Northern Russia. *CASP Rep. Arct. Russ. Stud. Reg. Arct. Proj.* **1997**, *663*, 146–150.
43. Dickinson, W.R.; Beard, L.; Brakenridge, G.R.; Erjavec, J.L.; Ferguson, R.C.; Inman, K.F.; Knepp, R.E.X.A.; Lindberg, F.; Ryberg, P.T. Provenance of North American Phanerozoic sandstones in relation to tectonic setting. *Bull. Geol. Soc. Am.* **1983**, *94*, 222–235.
44. Mange, M.A.; Maurer, H.F. *Heavy Minerals in Colour*; Chapman & Hall: London, UK, 1992; Volume 147, p. 145.
45. Morton, A.C.; Berge, C. Heavy mineral suites in the Statfjord and Nansen Formations of the Brent Field, North Sea; A new tool for reservoir subdivision and correlation. *Pet. Geosci.* **1995**, *1*, 355–364.
46. Galehouse, J.S. Point Counting. *Procedures in Sedimentary Petrology*; Wiley-Interscience: New York, NY, USA, 1971; pp. 385–407.
47. Sláma, J.; Kosler, J.; Condon, D.J.; Crowley, J.L.; Gerdes, A.; Hanchar, J.M.; Horstwood, M.S.A.; Morris, G.A.; Nasdala, L.; Norberg, N.; *et al*. Plesovice zircon—A new natural reference material for U-Pb and Hf isotopic microanalysis. *Chem. Geol.* **2008**, *249*, 1–35.
48. Paces, J.B.; Miller, J.D. Precise U-Pb ages of Duluth Complex and related mafic intrusions, northeastern Minnesota: Geochronological insights to physical, petrogenetic, paleomagnetic, and tectonomagmatic processes associated with the 1.1 Ga Midcontinent Rift System. *J. Geophys. Res. Solid Earth* **1993**, *98*, 13997–14013.
49. Hellstrom, J.; Paton, C.; Woodhead, J.; Hergt, J. Iolite: Software for spatially resolved LA-(quad and MC) ICPMS analysis. *Mineral. Assoc. Can. Short Course Ser*. **2008**, *40*, 343–348.
50. Paton, C.; Hellstrom, J.; Paul, B.; Woodhead, J.; Hergt, J. Iolite: Freeware for the visualisation and processing of mass spectrometric data. *J. Anal. Atom. Spectrom.* **2011**, *26*, 2508–2518.
51. Petrus, J.A.; Kamber, B.S. VizualAge: A novel approach to laser ablation ICP-MS U-Pb geochronology data reduction. *Geostand. Geoanal. Res.* **2012**, *3*, 247–270.
52. Pearce, N.J.G.; Perkins, W.T.; Westgate, J.A.; Gorton, M.P.; Jackson, S.E.; Neal, C.R.; Chenery, S.P. A compilation of new and published major and trace element data for NIST SRM 610 and NIST SRM 612 glass reference materials. *Geostand. Newslett.* **1997**, *21*, 115–144.

53. Lugwig, K. *Isoplot/Ex Version 4.1, a Geochronological Toolkit for Microsoft Excel*; Berkeley Geochronology Center Special Publication: Berkeley, CA, USA, 2010; No. 4
54. Smyth, H.R.; Hall, R.; Nichols, G.J. Significant volcanic contribution to some quartz-rich sandstones, east Java, indonesia. *J. Sediment. Res.* **2008**, *78*, 335–356.
55. Folk, R.L. *Petrology of Sedimentary Rocks*, 2nd ed.; Hemphill Press: Austin, TX, USA, 1974.
56. Dickinson, W.R.; Suczek, C.A. Plate tectonics and sandstone compositions. *Am. Assoc. Pet. Geol. Bull.* **1979**, *63*, 2164–2182.
57. Deer, W.A.; Howie, R.A. *An Introduction to the Rock-Forming Minerals*; Longman: New York, NY, USA, 1966.
58. Morton, A.C.; Hallsworth, C.R. Processes controlling the composition of heavy mineral assemblages in sandstones. *Sediment. Geol.* **1999**, *124*, 3–29.
59. Morton, A.C.; Hallsworth, C. Identifying provenance-specific features of detrital heavy mineral assemblages in sandstones. *Sediment. Geol.* **1994**, *90*, 241–256.
60. Gehrels, G. Detrital zircon U-Pb geochronology: Current methods and new opportunities. In *Tectonics of Sedimentary Basins: Recent Advances*; Busby, C., Pérez Azor, A., Eds.; John Wiley & Sons: Hoboken, NJ, USA, 2011; pp. 45–62.
61. Gehrels, G. Analysis Tools. Available online: http://www.geo.arizona.edu/alc/Analysis%20Tools.htm (accessed on 25 July 2013).
62. Corfu, F.; Hanchar, J.M.; Hoskin, P.W.O.; Kinny, P. Atlas of zircon textures. *Rev. Mineral. Geochem.* **2003**, *53*, 469–500.
63. Prokopiev, A.V.; Toro, J.; Miller, E.L.; Gehrels, G.E. The paleo–Lena River—200 m.y. of transcontinental zircon transport in Siberia. *Geology* **2008**, *36*, 699–702.
64. Bea, F.; Fershtater, G.; Montero, P. Granitoids of the Uralides: Implications for the evolution of the orogen. *Geophys. Monogr. Ser.* **2002**, *132*, 211–232.
65. Scarrow, J.; Hetzel, R.; Gorozhanin, V.; Dinn, M.; Glodny, J.; Gerdes, A.; Ayala, C.; Montero, P. Four decades of geochronological work in the southern and middle Urals: A review. *Geophys. Monogr. Ser.* **2002**, *132*, 233–255.
66. Brown, D.; Puchkov, V.; Alvarez-Marron, J.; Bea, F.; Perez-Estaun, A. Tectonic processes in the Southern and Middle Urals: An overview. *Geol. Soc. Lond. Mem.* **2006**, *32*, 407–419.
67. Görz, I.; Buschmann, B.; Kroner, U.; Hauer, R.; Henning, D. The Permian emplacement of granite–gneiss complexes in the East Uralian Zone and implications on the geodynamics of the Uralides. *Tectonophysics* **2009**, *467*, 119–130.
68. Marello, L.; Ebbing, J.; Gernigon, L. Basement inhomogeneities and crustal setting in the Barents Sea from a combined 3D gravity and magnetic model. *Geophys. J. Int.* **2013**, *193*, 557–584.
69. Lorenz, H.; Gee, D.G.; Simonetti, A. Detrital zircon ages and provenance of the Late Neoproterozoic and Palaeozoic successions on Severnaya Zemlya, Kara Shelf: A tie to Baltica. *Norw. J. Geol.* **2008**, *88*, 235–258.
70. Miller, E.; Gehrels, G.; Pease, V.; Sokolov, S. Stratigraphy and U-Pb detrital zircon geochronology of Wrangel Island, Russia: Implications for Arctic paleogeography. *AAPG Bull.* **2010**, *94*, 665–692.

71. Willner, A.P.; Sindern, S.; Metzger, R.; Ermolaeva, T.; Kramm, U.; Puchkov, V.; Kronz, A. Typology and single grain U/Pb ages of detrital zircons from Proterozoic sandstones in the SW Urals (Russia): Early time marks at the eastern margin of Baltica. *Precambrian Res.* **2003**, *124*, 1–20.
72. Pease, V.; Persson, S. Neoproterozoic Island Arc Magmatism of Northern Taimyr. In Proceedings of the Fourth International Conference on Arctic Margins, US Department of the Interior, Minerals Management Service OCS Study, Anchorage, AK, USA, October 2006; pp. 31–49.
73. Glodny, J.; Pease, V.; Montero, P.; Austrheim, H.; Rusin, A. Protolith ages of eclogites, Marun-Keu Complex, Polar Urals, Russia: Implications for the pre-and early Uralian evolution of the northeastern European continental margin. *Geol. Soc. Lond. Mem.* **2004**, *30*, 87–105.
74. Metelkin, D.V.; Vernikovsky, V.A.; Kazansky, A.Y.; Bogolepova, O.K.; Gubanov, A.P. Paleozoic history of the Kara microcontinent and its relation to Siberia and Baltica: Paleomagnetism, paleogeography and tectonics. *Tectonophysics* **2005**, *398*, 225–243.
75. Kuzmichev, A.B.; Pease, V.L. Siberian trap magmatism on the New Siberian Islands: Constraints for Arctic Mesozoic plate tectonic reconstructions. *J. Geol. Soc.* **2007**, *164*, 959–968.
76. Vernikovsky, V.A.; Pease, V.L.; Vernikovskaya, A.E.; Romanov, A.P.; Gee, D.G.; Travin, A.V. First report of early Triassic A-type granite and syenite intrusions from Taimyr: Product of the northern Eurasian superplume? *Lithos* **2003**, *66*, 23–36.
77. Massey, F.J., Jr. The Kolmogorov-Smirnov test for goodness of fit. *J. Am. Statist. Assoc.* **1951**, *46*, 68–78.
78. Glebovsky, V.; Kaminsky, V.; Minakov, A.; Merkur'ev, S.; Childers, V.; Brozena, J. Formation of the Eurasia Basin in the Arctic Ocean as inferred from geohistorical analysis of the anomalous magnetic field. *Geotectonics* **2006**, *40*, 263–281.
79. Malyshev, N.; Nikishin, V.; Nikishin, A.; Obmetko, V.; Martirosyan, V.; Kleshchina, L.; Reydik, Y.V. A New Model of the Geological Structure and Evolution of the North Kara Sedimentary Basin. *Doklady Earth Sci.* **2012**, *445*, 791–795.
80. Cawood, P.A.; Hawkesworth, C.J.; Dhuime, B. Detrital zircon record and tectonic setting. *Geology* **2012**, *40*, 875–878.
81. Grantz, A.; Hart, P.E.; Childers, V.A. Chapter 50 Geology and tectonic development of the Amerasia and Canada Basins, Arctic Ocean. *Geol. Soc. Lond. Mem.* **2011**, *35*, 771–799.
82. Miller, E.L.; Toro, J.; Gehrels, G.; Amato, J.M.; Prokopiev, A.; Tuchkova, M.I.; Akinin, V.V.; Dumitru, T.A.; Moore, T.E.; Cecile, M.P. New insights into Arctic paleogeography and tectonics from U-Pb detrital zircon geochronology. *Tectonics* **2006**, *25*, doi:10.1029/2005TC001830.
83. Amato, J.M.; Toro, J.; Miller, E.L.; Gehrels, G.E.; Farmer, G.L.; Gottlieb, E.S.; Till, A.B. Late Proterozoic–Paleozoic evolution of the Arctic Alaska–Chukotka terrane based on U-Pb igneous and detrital zircon ages: Implications for Neoproterozoic paleogeographic reconstructions. *Geol. Soc. Am. Bull.* **2009**, *121*, 1219–1235.